Thermodynamics and Hysteresis for Hydrogen Solution and Hydride Formation in Pd–Ni Alloys

Ted B. Flanagan and H. Noh

Department of Chemistry, University of Vermont Burlington, VT 05405, U.S.A.

Z. Naturforsch. **50a**, 475–486 (1995); received November 10, 1994

Pd and its fcc substitutional alloys which form hydride phases exhibit hysteresis. If Pd–Ni alloys have been hydrided and then dehydrided a number of times at a moderate temperature, the hysteresis is reduced. The reduction of hysteresis increases with increase of X_{Ni} to 0.15 and, if the $X_{Ni}=0.15$ alloy is hydrided and dehydrided (298 K) a number of times, hysteresis disappears. Hydrogen isotherms have been measured for annealed Pd–Ni alloys from $X_{Ni}=0.05$ to 0.25 (273 K). These show that the width of the plateau region decreases from $X_{Ni}=0$ to ≈ 0.15 and then increases again. This trend is not apparent from previous isotherm measurements but it is consistent with the x-ray results available in the literature. Thermodynamic parameters for hydrogen absorption/desorption have been measured in the dilute phase and in the plateau region.

Introduction

The Pd–Ni–H system has been investigated by several workers [1–5]. It is of especial interest because Ni also forms a hydride phase [6] which is isomorphous with the hydride of Pd and the limiting compositions of both hydrides are MH. Palladium and its Pd-rich alloys have a miscibility gap within which the hydride and dilute phases co-exist. The phase rule requires that under isothermal conditions the hydrogen pressure, the plateau pressure, is invariant when the two solid phases co-exist.

The hydrogen absorption behavior of palladium is modified by substitutional alloying [7]. For example, the plateau pressures increase with increase of X_{Ni} for homogenous solid solution Pd–Ni alloys. The results in the literature for the Pd–Ni–H system are conflicting because the isotherms [1, 2, 5] indicate that the hydrogen composition of the hydride phase decreases monotonically with X_{Ni} at least up to the $X_{Ni}=0.15$ alloy[1]. On the other hand, the lattice parameters of the co-existing dilute and hydride phases suggest that the width of the plateau region decreases to $X_{Ni}\approx 0.1$ and then increases again with X_{Ni} [5]. It would seem to be reasonable that the breadth of the plateau region would increase with Ni content from $X_{Ni}=0.1$, which is smaller than for Pd–H, because NiH is isomorphous with Pd–H; the reason for the initial decrease of the plateau breadth starting from Pd–H is unknown. The p_{H_2}-H-content relationship in the single β-phase region becomes less steep as X_{Ni} increases so that it becomes more difficult to locate the β-phase composition from the isotherms. Hopefully, by extending measurements to higher pressures and to higher Ni contents, the trends with X_{Ni} can be more readily established from the isotherms.

The palladium-hydrogen system exhibits substantial hysteresis and its most common manifestation is that the hydrogen pressure needed to form the hydride phase, p_f, is greater than the pressure needed for its subsequent decomposition, p_d. The magnitude of this isothermal hysteresis may be quantitatively expressed by the equation

$$\text{loss of useful energy due to hysteresis} = \tfrac{1}{2} RT \ln(p_f/p_d)\,. \quad (1)$$

Equation (1) is the minimum work which is done on the system which, under isothermal conditions, appears as heat in the surroundings. Thus isothermal hysteresis represents a loss of useful energy. For Pd–H there have been no reports of changes of hysteresis with cycling, i.e., with repeated hydriding and dehydriding at moderate temperatures, such as found for intermetallic compound hydrides [8].

The magnitude of hysteresis, (1), for an annealed $X_{Ni}=0.15$ alloy appears to be smaller [9] than for pure Pd–H; hysteresis has not been reported for alloys with $X_{Ni}>0.15$ and furthermore it has been found that

[1] The $X_{Ni}=0.2$ alloy–H system may have a broader plateau region than the lower content ones but it is difficult to discern this from the measured isotherms [5].

Reprint requests to Prof. T. B. Flanagan.

0932-0784 / 95 / 0400-0475 $ 06.00 © – Verlag der Zeitschrift für Naturforschung, D-72027 Tübingen

hysteresis disappears for an $Pd_{0.85}Ni_{0.15}$ alloy after a number of cycles of hydride formation and decomposition at moderate temperatures [9]. In this work the magnitudes of hysteresis and its disappearance with cycling will be examined for Pd–Ni alloys.

This research represents a continuation of research concerning a "second look" at the solubility of hydrogen in Pd-rich alloys where the Pd-alloy matrix can no longer be considered as an unchanging matrix [10]. Hydrogen-induced lattice changes are shown to affect the subsequent hydrogen solubilities.

Evidence for trapping by substitutional metals in palladium has not been found from hydrogen solubility studies but there is evidence from Mössbauer studies that for many disordered Pd-rich alloys the hydrogen avoids the octahedral interstices which have substitutional metal atoms as nearest neighbors [11]. It is generally believed that the interstitial sites which have only Pd atoms as nearest neighbors are the preferred ones in most Pd-rich alloys. Evidence for this is available from neutron diffraction studies on ordered Pd_3Mn where it was found that the octahedral sites with only Pd atom nearest neighbors (Pd_6) were 85% occupied and the (Pd_5Mn) sites were 15% occupied in $Pd_3MnD_{0.61}$ [12]. The fractions of the various types of octahedral interstitial sites in fully disordered, Pd-rich alloys can be calculated from the binomial distribution. Although the fraction of (Pd_6) sites is small in those alloys with large fractions of substituted metal, there is still no evidence from hydrogen solubility behavior, i.e., initial deviations from Sieverts' law, for hydrogen trapping in Pd-rich interstices at least over the temperature range where solubility studies can be readily carried out. Trapping is seen in heavily dislocated Pd where deviations from Sieverts' law occur as $r \rightarrow 0$ [13]. The fact that trapping does not seem to be a factor may be because the various site energies are not very different. In addition to the local effect of alloying which is due to different nearest neighbor environments of the interstices, alloying appears to also affect the hydrogen solubilities in a global way through electronic changes [7].

The dilute phase solubilities are of interest for probing the defect state of Pd and its alloys because this is generally more amenable to interpretation than data in the two phase region because of complications in the latter due to hysteresis. In view of the absence of evidence for trapping in the dilute phase solubilities, the hydrogen solubility for well-annealed Pd or disordered substitutional Pd alloys should follow Sieverts' law of ideal dilute solubility as $r=(H/M)\rightarrow 0$,

$$r = K_s\, p_{H_2}^{1/2}\,, \tag{2}$$

which is simply Henry's law for a dissociating gas. As the hydrogen contents in the dilute phase increase, the values of $p_{H_2}^{1/2}$ are generally lower than those predicted by Sieverts' law because of H–H attractive interactions. In the dilute phase of well-annealed Pd or its disordered substitutional alloys only this ideal solubility behavior, modified by the H–H interactions, should occur and therefore deviations from Sieverts' law can be attributed to lattice defects. This suggests that the dilute phase solubilities of hydrogen in alloys which have been cycled through the phase change may yield information about the nature of the defects introduced by the cycling process.

It is known that the tensile stress fields of edge dislocations in cold-worked Pd attract hydrogen; this leads to a hydrogen solubility enhancement in the dilute region of Pd–H and in Pd alloy–H systems, i.e., the solubility of hydrogen in cold worked samples is greater than in annealed ones at a given p_{H_2} [14–16]. Large dislocation densities are also created when the hydride phase forms and decomposes at moderate temperatures by cycling through the hydride phase change [17]. Consequently solubility enhancements found in cycled Pd are comparable to those observed in heavily cold-worked Pd [18]. The solubility enhancements in Pd have been calculated by considering the dislocation stress field interaction with the dissolved hydrogen [15, 19], however, the agreement can only be considered as semi-quantitative because the dislocation density is treated as an adjustable parameter.

In the higher hydrogen content region of the dilute phase of palladium, which has been previously cycled through the phase transition at moderate temperatures or else heavily wold-worked, the $p_{H_2}^{1/2}$ *versus* r relationship shows increasing curvature; the solubility data can no longer attributed to H segregation to the stress fields of edge dislocations [20]. In this higher concentration region the hydrogen solubility of Pd–H is irreversible and has therefore been attributed to the formation of the hydride phase before the normally expected value of p_f is reached. Little attention has been paid to this region of dilute solubilities in comparison to that given to the lower content, reversible region. The former irreversible dilute phase solubility also appears in other M–H systems including intermetallic–H ones after their activation by cycling [21].

For Pd and substitutional Pd–Ni alloys, which have been cycled through the hydride phase at moderate temperatures, the main cause for deviations from ideal dilute behavior is the presence of dislocation–H interactions [15]. Complex arrays of dislocations giving rise to long range internal stresses in heavily worked Pd may be the cause of the irreversibility observed at higher H contents in the dilute phase where hydride phase forms before the plateau. Long-range internal stress fields have been shown to exist in cold-worked fcc metals [22].

Segregation of the homogeneous alloys into regions which are inhomogeneous with respect to the metal atom concentrations due to cycling may also cause solubility enhancements in Pd alloys [23, 24].

Experimental

Pd–Ni alloys were prepared by arc-melting the pure components under argon several times with intermediate flipping of the buttons. The alloy buttons were then annealed for 2 d at 1173 K, rolled into thin foils and then reannealed for 2 d at 1173 K. The alloys were lightly abrading with fine emery paper and then cleaned ultrasonically with acetone before use. No difference was found in the dilute phase hydrogen solubilities between Pd–Ni alloys which had been rapidly quenched or else cooled slowly in a furnace; this behavior contrasts with Pd–Rh alloys where differences are observed [10]. This suggests that no concentration gradients develop during cooling the solid from elevated temperatures as might be expected from the continuous solid solubility reported in the phase diagram [25].

Three different forms of the lower content Ni alloys ($0 < X_{Ni} \leq 0.09$) were examined:

- annealed at 973 K for several days followed by a 1 h anneal at 1373 K,
- melt-spun, prepared by forcing the melt onto a rotating cooled copper wheel,
- cold-worked by rolling with several intermediate stress anneals. These alloys was not annealed after the arc-melting. The $X_{Ni} = 0.15$ alloy, however, was cold-rolled to 95% with an annealing treatment after arc-melting and without intermediate stress anneals.

The lower content alloys ($X_{Ni} \leq 0.09$) were analyzed by electron microprobe. The cold worked one showed the greatest compositional variations and the melt spun and annealed had comparable variations. For example, for the melt-spun $X_{Ni} = 0.092 \pm 0.003$ alloy, i.e., the standard deviation from the stated composition was ± 0.003 which presumably represents the maximum of compositional variations since the precision of analysis was considerably better than this. The compositions of these lower content alloys were all very close to their stated values, e.g., $X_{Ni} = 0.052 \pm 0.0025$. The compositions have been rounded off to: $X_{Ni} = 0.02$, 0.05 and 0.09. The higher composition alloys were prepared in our laboratory by arc-melting but without the detailed physical and compositional analyses as for the lower content ones.

Results and Discussion

Dilute Phase Solubilities

Dilute phase solubilities have been measured and thermodynamic parameters derived for hydrogen solution for some alloys in their annealed forms. The results are shown in Table 1 in comparison with earlier results.

The enthalpies are similar to those reported in the previous studies [5, 26] and, in fact, a good linear relationship obtains between ΔH_H^0 and X_{Ni} except the intercept at X_{Ni} appears to be somewhat too negative. The equation describing this dependence is

$$\Delta H_H^0/\text{kJ/mol}\,\tfrac{1}{2}H_2 = -11.2 + 34.8\,X_{Ni}\,. \qquad (3)$$

The entropies are nearly constant with X_{Ni} indicating that as $r \to 0$ all of the interstices can be occupied. It should be noted that it is important that the alloys be annealed and, for example, if they are cycled through the hydride phase change and then the dilute phase solubilities are then measured, the solubilities and

Table 1. A Summary of Some Dilute Phase Thermodynamic Parameters for Pd–Ni Alloys (298 K).

X_{Ni}	$-\Delta H_H^0$/kJ/mol H	$-\Delta S_H^0$ J/Kmol H
0	−10.5	−54
0.05	(−9.5)	(−55.3)
0.09	−8.2 (−7.9)	−58.0 (−55.9)
0.15	−5.8 (−6.0)	−58.1 (−55)
0.167	(−5.4)	(−56.9)
0.20	−4.4 (−4.5)	−58.3 (−54.5)
0.25	−2.3	−54.5
0.30	(−0.7)	(−52.2)

The values in parenthesis are from [5] except for the $X_{Ni} = 0.167$ alloy which is from [26].

derived thermodynamic parameters differ. The magnitudes of the relative partial molar enthalpies at infinite dilution steadily decrease with increase of X_{Ni} (Table 1); this accounts for the decrease in dilute phase hydrogen solubility at a given p_{H_2} with increase of X_{Ni}.

Complete Isotherms for Annealed Alloys

Hydrogen isotherms for annealed Pd–Ni alloys are shown in Fig. 1 (273 K), where an interesting trend is seen shown by the dashed curve, i.e., the hydrogen capacities decrease with increase of X_{Ni} and then increase again; the minimum appears at about $X_{Ni}=0.09$. The dashed curve has been drawn indicating the $(\alpha+\beta)/\beta$ phase boundary as judged from where the decomposition plateau commences. This behavior correlates with the dependence of $\Delta a = a_0^\beta - a_0^\alpha$ on X_{Ni} from [3] where a_0^β and a_0^α are the lattice parameters of the co-existing hydride and dilute phases, respectively. Hysteresis also shows a minimum between $X_{Ni}=0.09$ and 0.15 (Table 2) and a maximum near 0.05. The minimum in both hysteresis and Δa are attributed to the minimum in the hydrogen capacity but the reason for this minimum in capacity is not known.

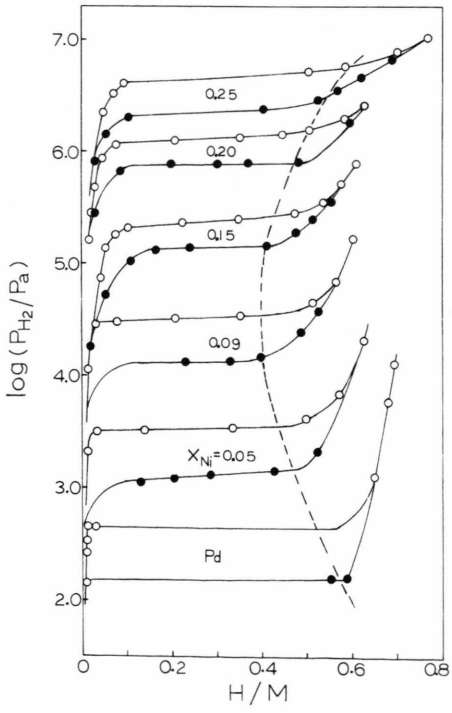

Fig. 1. Hydrogen isotherms for homogeneous fcc Pd–Ni alloys at 273 K. The open symbols are for absorption and the filled ones for desorption.

Table 2. A Summary of Effects of Cycling on Hysteresis ($\frac{1}{2}RT\ln(p_f/p_d)$ for Pd–Ni Alloys (initially annealed).

X_{Ni}	T/K	hyst. (annealed)/ J/mol H	hyst. (cycled)/ J/mol H
0	333	850	1000
0.02	303	889	940
0.05	303	985	1020
0.09	303	865	430
0.15	323	360	0
0.15	273	600	200 (3×)
0.20	273	650	220 (3×)
0.25	273	810	230 (3×)

The values in parenthesis indicate the number of cycles in those cases where not enough cycling was carried out to achieve limiting behavior.

The differences in behavior for the three different forms of the $X_{Ni}=0.09$ alloy are illustrated in Fig. 2 where a comparison is shown of their initial isotherms (303 K). It can be seen that the melt-spun and annealed forms have nearly identical isotherms but the cold worked one is more sloping. (This cold worked alloy was not annealed prior to rolling and therefore much of the sloping may be due to compositional inhomogeneities.) The subsequent isotherms of the melt-spun and annealed forms differ, however, with the latter having a significantly lower p_f and a higher p_d than the former form. The difference in behavior between these the various microstructural forms is found to be progressively smaller for the alloys with $X_{Ni}=0.05$ and 0.02.

Thermodynamic properties were determined for the $X_{Ni}=0.09$ alloy from van't Hoff plots and from reaction calorimetry. The latter data are shown in Fig. 3 where it can be seen that the enthalpy for hydride formation and decomposition are equal and their magnitudes are 14.9 kJ/mol $\frac{1}{2}H_2$. This is equal to the average of the values from the van't Hoff plots for p_f and p_d; the problems of obtaining data from van't Hoff plots for this alloy have been discussed elsewhere as representative of a general problem when the plateau pressures of alloys change due to cycling [27]. The calorimetric enthalpy change is less than that for Pd–H which is 19.2 kJ/$\frac{1}{2}H_2$ [28]. The ratio of the average of the average of the plateau pressures, $((p_f+p_d)/2$, for the $X_{Ni}=0.09$ alloy and for Pd expressed as the free energy change is

$$\tfrac{1}{2}RT\ln[p_{av}(\mathrm{Pd})/p_{av}(X_{Ni}=0.09)] = 4.04\ \mathrm{kJ/mol}\ \tfrac{1}{2}H_2. \quad (4)$$

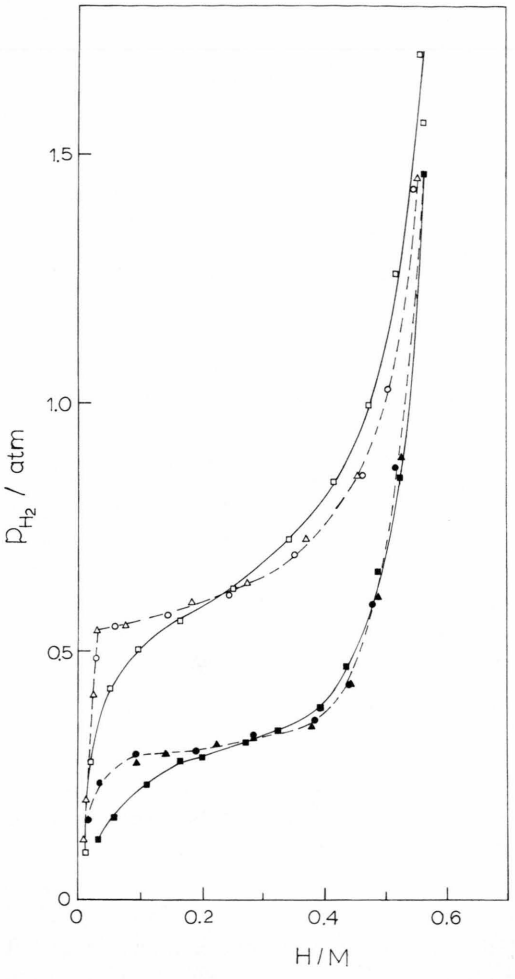

Fig. 2. Isotherms for three different forms of the $X_{Ni}=0.9$ alloy at 303 K. □, cold-rolled; △, annealed; ○, melt-spun.

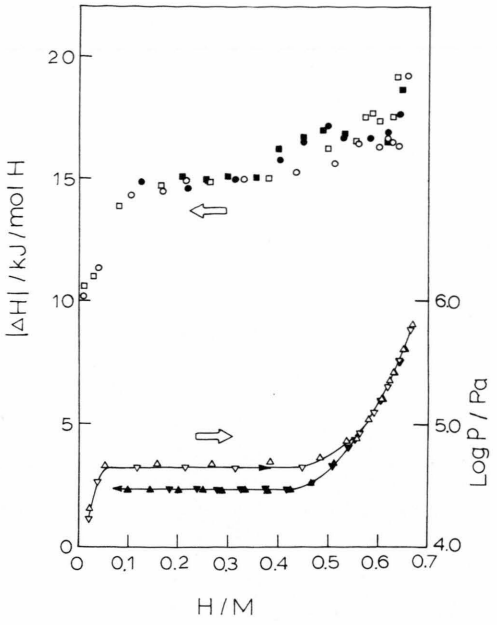

Fig. 3. Reaction calorimetric data for the $X_{Ni}=0.09$ alloy at 298 K. The difference between the absorption and the desorption data for (H/M) values >0.4 is due to hysteresis and should not be attributed to scatter. ○, □, ΔH; △, ▽, p_{H_2} data. The open symbols are for absorption and the filled ones for desorption.

This value is quite close to the difference in the calorimetric enthalpies of 4.3 kJ/mol $\frac{1}{2}H_2$ indicating that the plateau entropy values are quite similar. There is no clear indication that the magnitudes of the enthalpies decrease in the high H content single hydride phase region as they do for Pd–H [28]. This is the reason that the increase of p_{H_2} with r is not so steep for these alloys as for Pd–H. This is presumably a result of the electronic structures of these alloys.

Complete isotherms were measured at a series of temperatures for both H_2 and D_2 for the $X_{Ni}=0.02$, 0.05 and 0.09 after they had been cycled. A typical comparison is shown in Figure 4 for the 0.09 alloy at 323 K. The dashed line shows pressures for H_2 after having been multiplied by a factor of 4.0 which is a similar factor needed for pure Pd–H(D). It can be seen in Fig. 4 that the isotope effect is nearly constant over the whole range of contents. The isotope effect appeared to be the same for all of the Ni compositions investigated.

Effect of Cycling on the Dilute Phase Solubility

The results of cycling on the dilute phase hydrogen solubility for pure Pd (333 K) are shown in Figure 5. (It will be shown below that the plateau pressure p_f increases slightly with cycling.) The initial isotherm cycle exhibits supersaturation of the dilute phase since the data point shown above the plateau pressure is metastable for times longer than the laboratory scale. The supersaturation is not observed in subsequent cycles nor is it observed in the Pd–Ni alloys except perhaps for a small trace in the lowest Ni content one. The first cycle causes the largest effect on the solubility and small increases continue until stable behavior is reached between the second and ninth cycles.

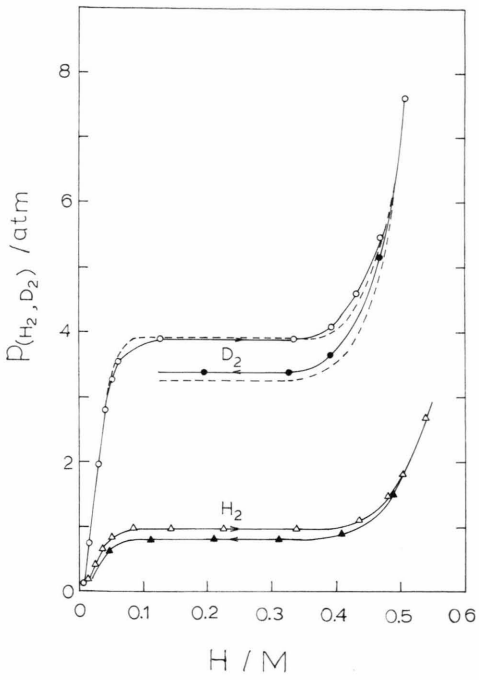

Fig. 4. Isotherms for the $X_{Ni}=0.09$ alloy (cycled) at 323 K for H_2 and D_2. The dashed line has been obtained by multiplying the data for H_2 by a factor of 4.

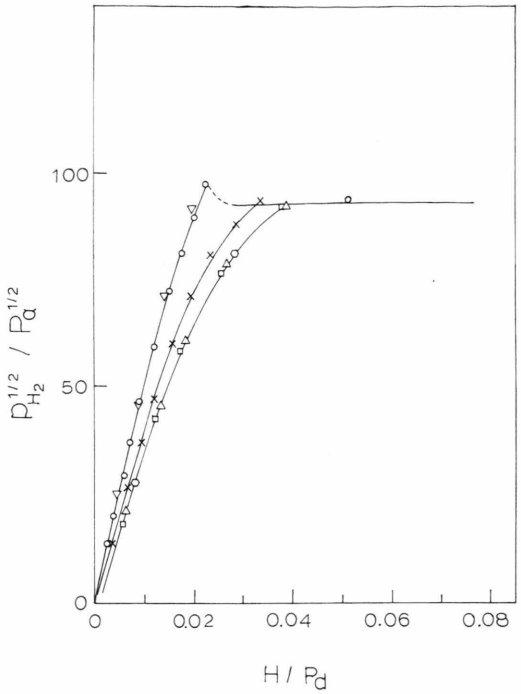

Fig. 5. Dilute phase isotherms for Pd–H (333 K) as a function of cycling completely through the hydride phase at 333 K and then dehydriding at the same temperature. ○, first cycle; ×, second cycle; □, ninth cycle; △, twentyfirst cycle; ▽, after annealing the sample which had been cycled 21 times for 12 h at 693 K; ○, after cycling the sample annealed at 693 K for 4×.

Dilute phase solubilities of the $X_{Ni}=0.09$ alloy, which was initially in its annealed form, are shown in Fig. 6 for consecutive cycles of hydride formation and decomposition where the dilute solubility increases continuously up to about 5 cycles after which the solubility no longer appears to change. These increases of solubility are accompanied by concomitant decreases of p_f and its value becomes constant after about 5 or 6 cycles. It seems that the changes of the dilute phase solubility and the plateau pressure caused by cycling are related for the alloys but for Pd–H the dilute phase solubility continues to increase with cycling while p_f does not change after a small increase.

Thermodynamic parameters for hydrogen solution were evaluated from the dilute phase isotherms for the $Pd_{0.91}Ni_{0.09}$ alloy after cycling six times at 303 K and the results at infinite dilution are: $\Delta H^0_H = -12.0$ kJ/mol $\frac{1}{2}H_2$ and $\Delta S^0_H = -68.3$ J/K mol $\frac{1}{2}H_2$. The enthalpy for this cycled alloy is more exothermic and the entropy more negative than for the annealed alloy form (Table 1) indicating that the cycled alloys contain defect sites which are more energetic for hydrogen occupation than are the normal interstices found in annealed alloys. From these results it seems clear that cycling leads to a somewhat different microstructure in the Pd–Ni alloys as compared to pure Pd and the difference increases with X_{Ni}. It has been observed that the Pd–Ni alloys work harden more than several other Pd alloys which have been examined [29], e.g., Pd–Co or Pd–Cr, and this may contribute to the creation of large long-range stress fields.

For cycled or heavily cold worked Pd and Pd alloy–H systems the solubility behavior becomes irreversible in the dilute phase as the two phase, plateau pressure is approached [20]. This irreversibility has been attributed to hydride formation in stressed regions of the metal where hydride phase forms more readily than in the bulk of the metal due to tensile stress [20]. This irreversibility in the dilute phase only appears after cycling the alloys through the hydride phase or else after heavy cold-work. (It had been reported [20] that irreversibility occurs only for cycled and not for cold-worked Pd but this was due to the

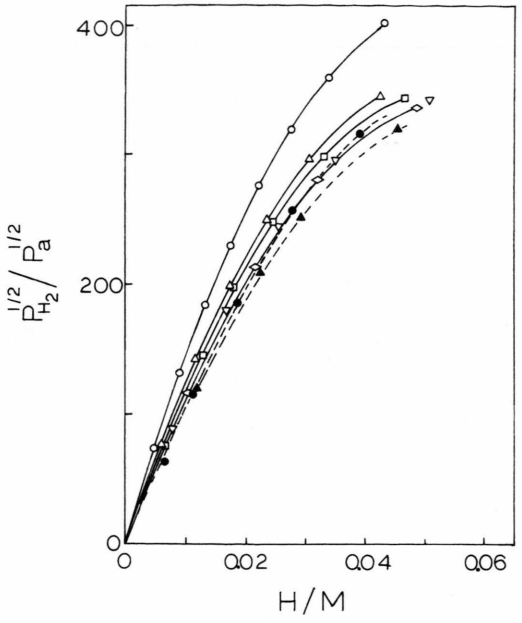

Fig. 6. Dilute phase isotherms for the $X_{Ni}=0.09$ alloy at 323 K as a function of cycling, i.e., completely forming and decomposing the hydride phase at 323 K. ○, first cycle; △, second cycle; □, third cycle; ▽, fourth cycle; ◇, fifth cycle; A cold-rolled alloy (95%) is also shown. ●, first cycle; ▲, second cycle.

fact that the degree of cold work was not extensive enough.) It does not seem likely that these stresses are from the stress fields about isolated dislocations because in cold-worked Pd at $r=0.0085$ inelastic neutron scattering experiments lead to the result that the frequencies correspond to the dilute, rather than hydride phase even though the concentration is quite large around the dislocations [30]. It seems more likely that this type of irreversibility arises from the long-range internal stress fields arising from complex dislocation arrays [22] rather than from individual edge dislocation–H interactions because the volume extent of the latter may be too small to form a hydride phase. The inelastic scattering measurements, which were carried out at $r=0.0085$ (presumably at 298 K) [30], should also be carried out at, e.g., $r=0.012$ where curvature and irreversibility are found in the dilute phase solubility of heavily cold worked Pd [20].

An interesting result is shown in Fig. 7 for the $X_{Ni}=0.15$ alloy where, in contrast with the dilute phase behavior for Pd–H, after the first cycle of hydriding the dilute phase solubility is reversible in the region where the solubility shows much curvature and the transition to the two phase region is very gradual rather than sharp (Figure 7). The filled symbols show the desorption during the second and third cycles and both represent an incremental loss of hydrogen of ≈ 0.015; for comparison the desorption data for the second cycle of Pd–H exhibits considerable irreversibility. This absence of irreversibility in the very curved part of the dilute phase solubility of the $X_{Ni}=0.15$ alloy does not indicate the absence of hydride formation but the disappearance of hysteresis which is consistent with its absence in the plateau region. This indicates that the hysteresis in the main plateau region and in the dilute phase are both caused by hydride formation and decomposition.

Effect of Cycling on Plateau Pressures

The effects of cycling on the plateau pressures of the Pd–Ni alloys depends upon the alloy composition and the temperature. Generally the effect of cycling is greater, the larger is X_{Ni} (Table 2). Except for Pd and

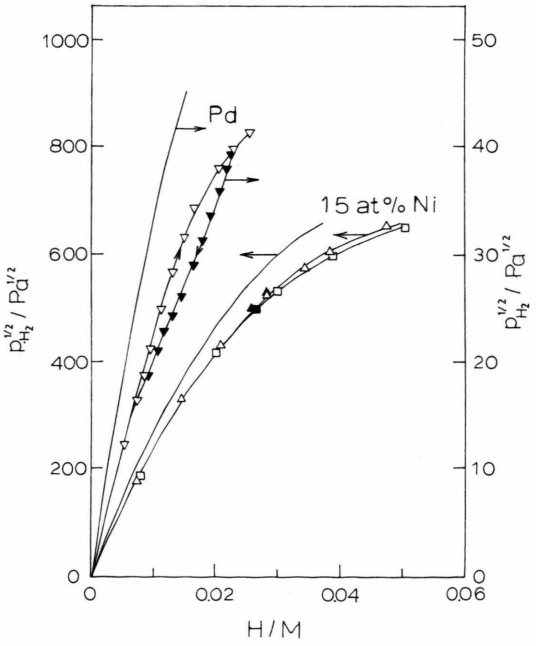

Fig. 7. Dilute phase solubility for Pd–H (298 K, right-hand scale) and $Pd_{0.85}Ni_{0.15}$–H (303 K, left-hand scale) showing irreversible and reversible behavior for the former and the latter, respectively. The continuous curves without data points are for the annealed samples and both are reversible. ▽, Pd second cycle; △, □, second and third cycles for the $Pd_{0.85}Ni_{0.15}$ alloy. The open symbols are for absorption and the filled ones for desorption.

the alloy with lowest Ni content, the effect of cycling is to decrease p_f and increase p_d. The cycling results at 323 K are shown in Figs. 8 to 11 for $X_{Ni}=0.0$, 0.05, 0.09 and 0.15 alloys. Some cycling of the 0.20 and 0.25 alloys was also carried out (273 K) but since the establishment of equilibrium was rather slow, these alloys were cycled only 3 × and probably did not reach their final plateau values. It can be seen from Table 2 that hysteresis for the annealed form of each alloy increases with X_{Ni}, decreases and then again increases.

Although it would have been anticipated that the effect of cycling on pure Pd–H would have been already reported in the literature, the authors are unaware of any data showing explicitly the changes of plateau pressures with cycling. The plateau pressures, p_f, of Pd–H progressively increase and then appear to stabilize; p_d does not change very much (Figure 8). This cycling of pure Pd has been carried out at 303 and 393 K with the same results except that they show that the higher, stable value of p_f is reached at 303 K after 3 or 4 cycles and at 393 K it is reached after the second cycle. If the cycled Pd is annealed at as relatively low temperature, 693 K for 12 h, the value of p_f returns to that of Pd which had been annealed at 1173 K; after the fourth cycle of hydriding/dehydriding, p_f returns to the higher value found after the previous cycling (Figure 8).

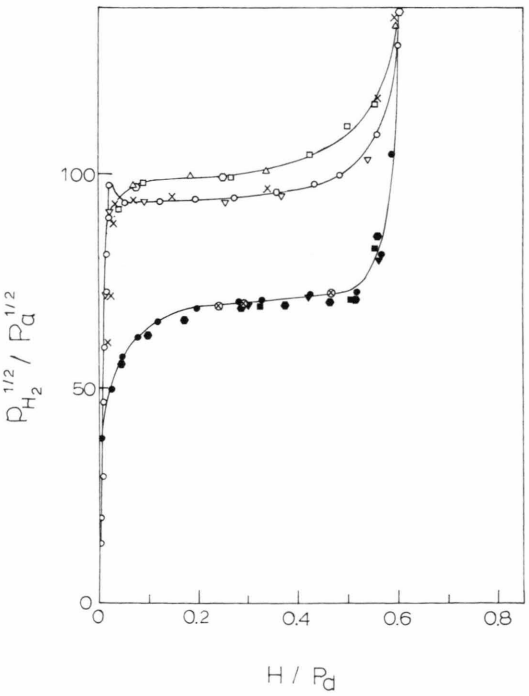

Fig. 8. The effect of cycling on the complete isotherms for initially annealed Pd at 333 K. ○, initial cycle showing supersaturation of the α-phase; ×, ⊗, absorption and desorption data for the second cycle; ○, ninth cycle; □, 21st cycle; ▽, after annealing for 12 h at 693 K; △, after fourth cycle following annealing at 693 K. The open symbols, except for ⊗, are for absorption and the filled ones for desorption.

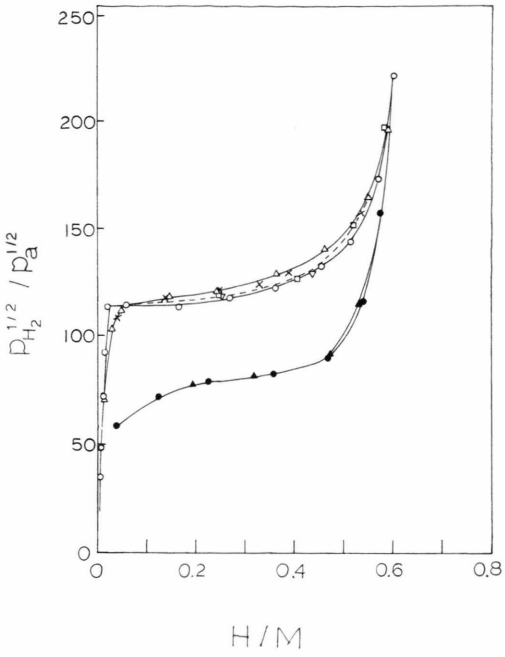

Fig. 9. The effect of cycling on the complete isotherms for initially annealed $Pd_{0.95}Ni_{0.05}$ at 303 K. ○, initial cycle; △, second cycle; ×, third cycle; □, fourth cycle; ▽, fifth cycle. The open symbols are for absorption and the filled ones for desorption.

The plateau pressure of the $X_{Ni}=0.02$ alloy (annealed) increases and then decreases again with cycling; these changes are small and are not shown. The value of p_f for the 0.05 alloy (annealed) initially increases and then decreases to a value lower than its initial one; its p_d value increases but these latter changes are small and not apparent in Figure 9. The observed plateau pressure changes are larger for the $X_{Ni}=0.09$ and 0.15 alloys than for alloys with smaller Ni contents and the p_f values of these higher Ni content alloys no longer increase initially (Fig. 10) as for the lower Ni content alloys (Figs. 8 and 9) but they continually decrease and then stabilize. The $X_{Ni}=0.09$ alloy was cycled in more than 4 different forms/preparations, i.e., annealed, remelted and re-annealed, melt-spun, and a different preparation of the alloy in annealed form. The details of the cycling behavior differ

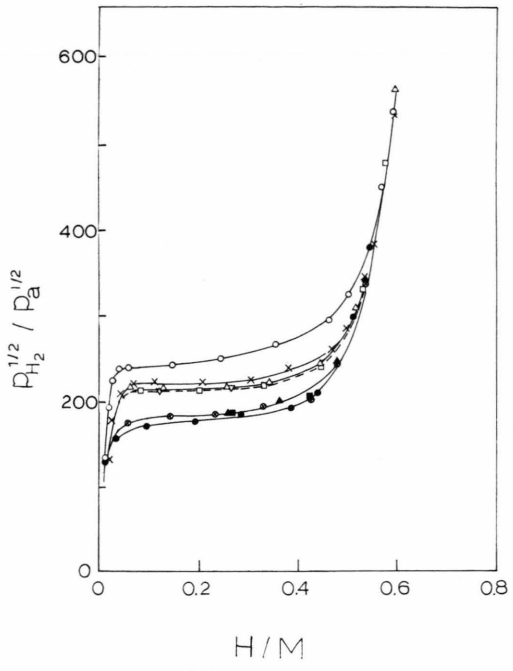

Fig. 10. The effect of cycling on the complete isotherms for a melt-spun $Pd_{0.91}Ni_{0.09}$ alloy at 303 K. ○, initial cycle; ×, ⊗, absorption and desorption data for the second cycle; △, third cycle; □, fourth cycle; ▽, fifth cycle. The open symbols are for absorption and the filled ones for desorption

but the trends are all similar. Figure 10 shows cycling of the melt-spun form at 303 K. The value of p_d increases after the second cycle and then stabilizes whereas the value of p_f decreases and stabilizes after about 4 or 5 cycles. The annealed forms show a similar behavior with cycling and therefore the grain size, which is small for the melt-spun form, does not play a decisive role in the cycling behavior.

(The cycling for the $X_{Ni}=0.15$ alloy is not shown because it was shown in the preliminary report showing the disappearance of hysteresis [9]). The $X_{Ni}=0.15$ alloy exhibited dramatic changes as a result of cycling; the hysteresis decreased from 360 J/mol H to essentially zero after 7 or 8 cycles at 323 K [9].

These data show that the plateau pressures of Pd–Ni alloys, and the accompanying hysteresis, change markedly with repeated formation and decomposition of the hydride phase at moderate temperatures (Fig. 10 and Ref. [9]). Except for two brief reports [9, 24], this has not been previously reported despite the very large number of isotherm measurements of Pd alloys and it has been generally assumed that the plateau pressures are invariant for a given form of the alloy. These changing plateaux have ramifications for the practical uses of these materials where their use may depend on specific plateau pressures.

Effect on the Isotherms of Cold-work Followed by Cycling

The results of cold-working and subsequent cycling on the $X_{Ni}=0.15$ alloy were investigated at 323 K and found to be surprising. In contrast to the cold worked alloy shown in Fig. 2, this alloy was annealed after arc-melting and then cold-rolled to 95% deformation, where $(d-d_0)/d_0 \times 100\% = 95\%$. For the cold-rolled alloy both p_f and p_d values were found to be lower than for its annealed form and, in addition, the hysteresis was smaller, i.e., 175 compared to 360 J/mol H; the plateaux were noticeably shorter and flatter than those for the annealed form of the alloy (Figure 11).

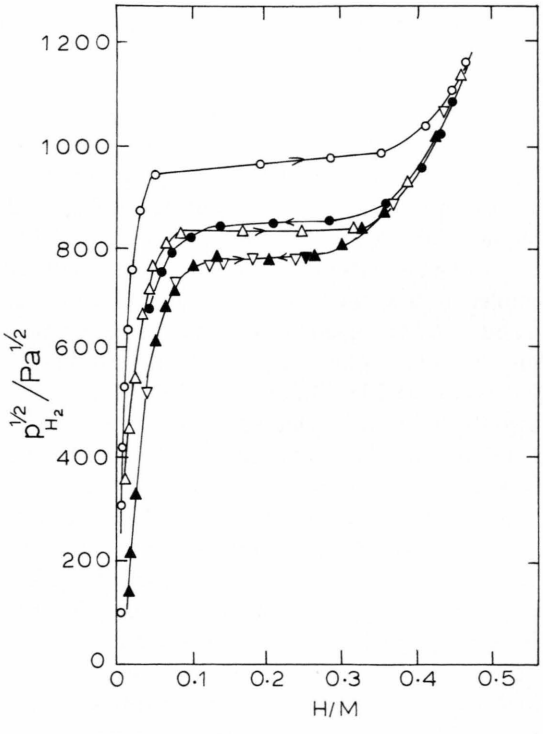

Fig. 11. The effect of cold-rolling and subsequent cycling on the isotherms of a $Pd_{0.85}Ni_{0.15}$ alloy at 323 K. ○, isotherm for an annealed alloy of the same composition; △, isotherm for the cold-rolled alloy; ▽, isotherm for the second cycle of the cold-rolled alloy. The open symbols are for absorption and the filled ones for desorption.

For the second hydriding cycle of this cold-rolled alloy, the value of p_f decreased to the p_d value eliminating the hysteresis (Figure 11).

Thus for the cold worked alloy both plateau pressures are reduced so that p_f is lower than the value of p_d for the annealed form of the alloy and for the second cycle, hysteresis is completely eliminated (Figure 11). This is a noteworthy result because the cold-working/cycling causes the equilibrium transition to shift to lower hydrogen chemical potentials compared to the annealed form, i.e., the changes are not restricted to changes of hysteresis. By contrast, cold-working has only a minimal effect on the plateau pressures of pure Pd [20].

The Recovery of the Cycled $Pd_{0.85}Ni_{0.15}$ Alloy by Annealing in vacuo

A $X_{Ni}=0.15$ alloy was cycled until hysteresis disappeared; it was then annealed *in vacuo* at progressively higher temperatures to learn about the disappearance of the effects of cycling. The progress of the annealing was followed by changes (323 K) of the hydrogen solubility enhancement in the dilute phase and the plateau pressure for hydride formation, p_f, at various stages of the annealing. The annealing was cumulative, i.e., progressively higher temperatures were employed with the same sample, and generally each period of annealing was for about 12 h. Figure 12 shows the solubilities in the very dilute phase at 323 K after annealing at various temperatures. The recovery is complete in the very dilute phase after annealing at 873 K but still incomplete in the higher content region within the dilute phase, e.g., $r>0.01$, and in the plateau region. In Fig. 13 values of p_f (323 K) are plotted against the annealing temperature where it can be seen that the alloy does not return to its initial p_f value after annealing at 873 K. The recovery of values of (r'/r) and p_f both commence at about 523 K and continue to $\approx$923 K where no further changes are observed. The recovery was about the same in the presence of 50 bar of $H_2(g)$ or *in vacuo*. The recovery takes place over a slightly higher temperature range than the recovery of the solubility enhancement in cold worked palladium or the $X_{Ag}=0.05$ substitutional Pd alloy [16]. Presumably the annealing treatment progressively rearranges and reduces the dislocation density which gives rise to the solubility enhancements and therefore the very dilute phase solubility recovers completely. In the higher content dilute phase, however, the recovery is incomplete after annealing at 923 K because some remaining long range, although small, stresses hydride phase to form.

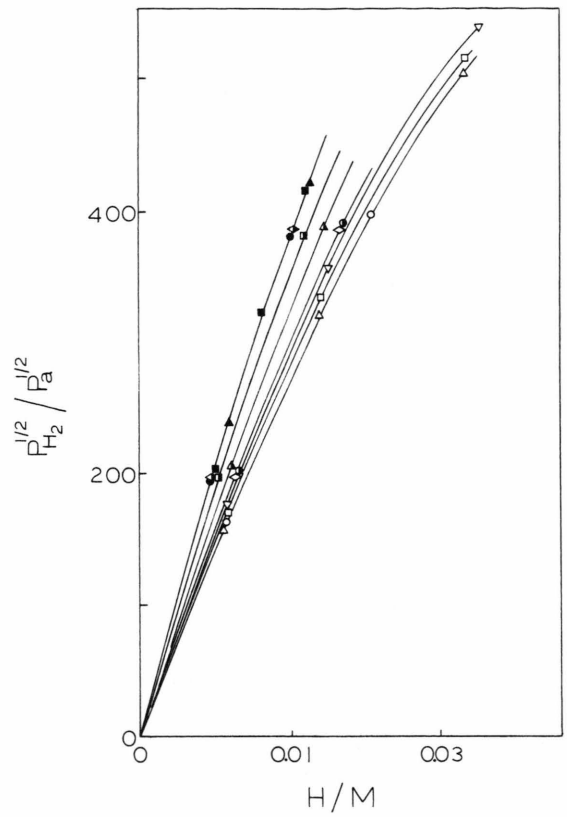

Fig. 12. The effect of progressively higher annealing temperature on the very dilute phase solubility of a $Pd_{0.85}Ni_{0.15}$ alloy (323 K) which had been cycled (8 × at 303 K). The temperatures are the annealing temperatures for $\approx$12 h periods *in vacuo*. ■, before cycling (annealed at 1173 K, 2 d); ○, isotherm after cycling; △, 473 K; □, 523 K; ▽, 673 K; ◇, 623 K; □, 673 K; △, 723 K; □, 773K; ◇, 823 K; ●, 873 K; ▲, 923 K.

The recovery of a $X_{Ni}=0.15$ alloy which had been cold-rolled and then cycled until hysteresis disappeared was progressively annealed. In the temperature range from 523 to 673 K hysteresis remained negligible and the plateau pressure ($p_f=p_d$) progressively increased with the annealing temperature. Hysteresis reappared after annealing at temperatures above 673 K. In the dilute phase the solubility enhancement decreased steadily in the temperature range from 523 to 673 K. Both of these monitors of the recovery showed a jump in the extent of recovery between 673 and 773 K.

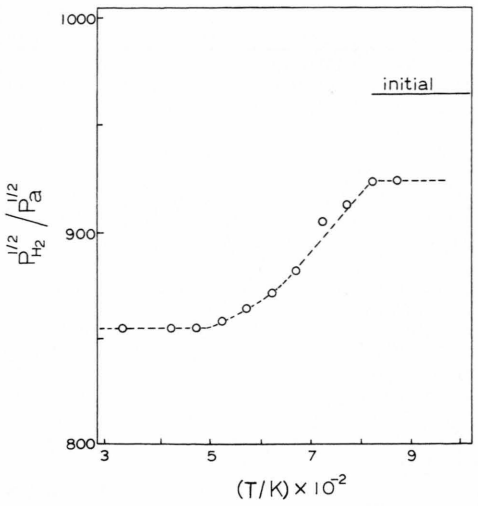

Fig. 13. The effect of progressively higher annealing temperatures on the plateau pressures for hydride formation measured at 323 K ($r=0.21$) for a $Pd_{0.85}Ni_{0.15}$ alloy which had been cycled (8× at 303 K).

The Reduction of Hysteresis by Cycling

One of the main results is the observation of the reduction of hysteresis with cycling of Pd–Ni alloys; the reduction culminates in the disappearance of hysteresis after about 7 cycles in the $X_{Ni}=0.15$ alloy–H system (323 K). A closely related result is that hysteresis disappears after only one cycle for an initially cold-rolled (95% deformation) $X_{Ni}=0.15$ alloy and the single plateau shifts to a lower pressure than either plateau of the annealed alloy. These results may provide clues to the origin of hysteresis in Pd and its alloys. The elimination of hysteresis is a result of microstructural changes in the alloy resulting from cycling and/or cold working. It should be recalled that hysteresis for Pd–H increases slightly as a result of cycling but is unaffected by cold-working.

Hysteresis is not eliminated by cycling a $X_{Ni}=0.09$ alloy (303 K) but is significantly reduced. It was found by comparison with the isotherms for a virgin, annealed alloy that the reduction of the hysteresis depends markedly on the temperature [27]. At 343 K the reduction was very large where hysteresis was only 17% of that for the annealed form but at 273 K, it was 57% of the annealed form. It is quite likely that hysteresis may be significant for the cycled $X_{Ni}=0.15$ alloy below 323 K; it was observed to be appreciable after 3 cycles at 273 K.

The following experiment with the $X_{Ni}=0.09$ alloy was carried out to learn about the origins of the cycling effect. The hydride phase was prepared by passing around the miscibility gap (T_c is estimated as ≈ 393 K). The hydride phase was then decomposed at 323 K; the decomposition pressure, p_d, was found to be the same as found when the hydride phase was formed in the usual way at 323 K by passing through the miscibility gap. Thus it seems that the presence of dislocations from hydride formation does not affect the value of p_d.

In multiple interface martensitic systems elastic energy can be stored; this storage is reflected during the hysteresis cycle by the decreasing temperatures (larger driving force) needed for the transformation, with fraction of conversion of the parent to the martensite phase [31]. The reverse transformation starts at a relatively low temperature but this increases with the fraction of transformation. For metal hydrides storage of elastic energy would correspond to sloping pressure plateaux. Since the plateaux generally become more horizontal with cycling, it does not seem likely that elastic energy plays an important role.

Acknowledgements

TBF wishes to dedicate this paper to Professor E. Wicke with affection and great respect. We thank the N.S.F. and Los Alamos National Laboratory (University of California) for financial support of this research. We especially wish to thank Sherri Bingert of Los Alamos National Laboratory for preparation and characterization of the Pd–Ni alloys (up to 9 atom %Ni). Da Wang and Suifang Luo are thanked for their assistance in some of the experiments.

[1] J. Barton, J. Green, and F. Lewis, Trans. Faraday Soc. **62,** 960 (1966).
[2] J. Green and F. Lewis, Trans. Faraday Soc., **62,** 971 (1966).
[3] Y. Sakamoto, K. Yuwasa, and K. Hirayama, J. Less-Common Mets., **88,** 115 (1982)
[4] V. Antonov, T. Anonova, I. Belash, E. Ponyatovskii, V. Rashupkin, and V. Thiessen, phys. stat. sol. **77a,** 71 (1983).
[5] Y. Sakamoto, T. Matsuo, H. Sakai, and T. B. Flanagan, Z. Physik. Chem. N.F. **162,** 83 (1989).
[6] B. Baranowski and K. Bochénska, Roczn. Chemii. **38,** 1419 (1964).
[7] E. Wicke and H. Brodowsky, in: Hydrogen in Metals vol. 2, G. Alefeld, J. Völkl, Springer-Verlag, Berlin 1978, p. 73
[8] W. Luo, J. Clewley, and T. Flanagan, Z. Physik. Chem. N.F. **179,** 83 (1993).
[9] H. Noh, T. Flanagan, Z. Gavra, J. Johnson, and J. Reilly, Scripta Met. et Mat. **25,** 2177 (1991).
[10] H. Noh, W. Luo, and T. Flanagan, J. Alloys and Compounds **196,** 7 (1993).
[11] F. Wagner, M. Karger, F. Pröbst, and B. Schüttler, in: NATO Series on Materials Science, P. Jena, C. Satterthwaite, eds., Plenum Publ. Col., New York 1983, p. 581.
[12] A. Ahlzén, Y. Andersson, R. Tellgren, D. Rodic, T. Flanagan, and Y. Sakamoto, Z. Physik. Chem. N.F. **163,** 213 (1989).
[13] S. Kishimoto and T. B. Flanagan, in: NATO Series on Materials Science, P. Jena, C. Satterthwaite, eds., Plenum Pub. Co., New York 1983, p. 623.
[14] T. Flanagan, J. Lynch, J. Clewley, and B. von Turkovich, J. Less-Common Mets. **49,** 13 (1976).
[15] R. Kirchheim, in: Prog. Mater. Sci. **32,** 261 (1988).
[16] S. Kishimoto, N. Yoshida, Y. Arita, and T. Flanagan, Ber. Bunsenges. Physik. Chem. **44,** 612 (1990).
[17] M. Wise, J. Farr, I. Harris, and J. Hirst, L'Hydrogene dans les Metaux Paris: Editions Science et Industrie, **Vol. 1** (1977), p. 1.
[18] J. Lynch, J. Clewley, T. Curran, and T. Flanagan, J. Less-Common Mets. **55,** 153 (1977).
[19] W. Wolfer and M. Baskes, Acta Met. **33,** 2005 (1985).
[20] T. Flanagan, S. Kishimoto, and G. Biehl, Chemical Metallurgy – A Tribute to Carl Wagner, N. Gokcen, ed., Met. Soc. A.I.M.E. 471 (1981).
[21] B. Bowerman, C. Wulff, G. Biehl, and T. Flanagan, J. Less-Common Mets. **73,** 1 (1980).
[22] H. Mughrabi, Acta Met. et Mat. **31,** 1367 (1983).
[23] H. Noh, T. Flanagan, and M. Ransick, Scripta Met. et Mat. **26,** 353 (1992).
[24] H. Noh, T. Flanagan, B. Cerundolo, and A. Craft, Scripta Met. et Mat. **25,** 225 (1991).
[25] M. Hansen, Constitution of Binary Alloys, McGraw-Hill, New York 1958.
[26] H. Brodowsky and H. Husemann, Ber. Bunsenges. Physik. Chem. **70,** 626 (1966).
[27] H. Noh, S. Luo, D. Wang, J. Clewley, and T. Flanagan, J. Alloys and Compounds, Submitted.
[28] T. Flanagan, W. Luo, and J. Clewley, J. Less-Common Mets. **172–174,** 42 (1991).
[29] S. Bingert, Los Alamos National Laboratory, Private Communication (1993).
[30] X. Huang, H.-D. Carstanjen, J. Rush, and R. Kirchheim, in: Proc. NATO Adv. Workshopin "Chemistry and Physics of Fracture" NATO ASI Ser. Ser. E, 580 (1987).
[31] R. Salzbrenner and M. Cohen, Acta Met. **27,** 739 (1973).